

This is the accepted manuscript made available via CHORUS. The article has been published as:

Effect of Drift Waves on Plasma Blob Dynamics

Justin R. Angus, Maxim V. Umansky, and Sergei I. Krasheninnikov

Phys. Rev. Lett. **108**, 215002 — Published 23 May 2012

DOI: [10.1103/PhysRevLett.108.215002](https://doi.org/10.1103/PhysRevLett.108.215002)

Effect of Drift Waves on Plasma Blob Dynamics

Justin R. Angus,¹ Maxim V. Umansky,² and Sergei I. Krasheninnikov¹

¹*University of California, San Diego*

²*Lawrence Livermore National Lab*

(Dated: March 26, 2012)

Abstract

Most of the work to date on plasma blobs found in the edge region of magnetic confinement devices is limited to 2D theory and simulations which ignore the variation of blob parameters along the magnetic field line. However, if the 2D convective rate of blobs is on the order of the growth rate of unstable drift waves, then drift wave turbulence can drastically alter the dynamics of blobs from that predicted by 2D theory. The density gradients in the drift plane that characterize the blob are mostly depleted during the nonlinear stage of drift waves resulting in a much more diffuse blob with a greatly reduced radial velocity. Sheath connected plasma blobs driven by effective gravity forces are considered in this paper and it is found that the effects of resistive drift waves occur at earlier stages in the 2D motion for smaller blobs and in systems with a smaller effective gravity force. These conclusions are supported numerically by a direct comparison of 2D and 3D seeded blob simulations for magnetic field curvature and gradient driven blobs.

Coherent structures having isolated density bumps in the drift plane and extended along the magnetic field, known as plasma blobs, are formed as a result of turbulent fluctuations in magnetic confinement devices and can often dominate the cross field transport in the edge region between the confined plasma and material surfaces. Plasma blobs are of considerable interest for a better understanding of edge transport and plasma exhaust in future toroidal fusion devices and have drawn significant attention from the physics community in recent years [1–15]. A thorough review of the current theoretical and experimental understanding of plasma blobs is given in [13].

The basic physics of blobs, shown in Fig. 1, is that charge polarizing forces combined with a vertical density gradient result in an electric field that drives the blob radially outward due to $\mathbf{E} \times \mathbf{B}$ convection [1]. The electric potential ϕ is limited by charge mitigation through the parallel dynamics which for sheath connected blobs is the flow of current into the sheaths. In this paper, we consider sheath connected plasma blobs driven by effective gravity forces that can be described by a local slab geometry with x the effective radial coordinate, y the effective poloidal coordinate, and z follows the magnetic field \mathbf{B} . In toroidal devices, this model represents blobs in the outer midplane where the toroidal magnetic field is typically much larger than the poloidal field. A discussion of the limitations of this model and a review of other blob models can be found in [10, 13].

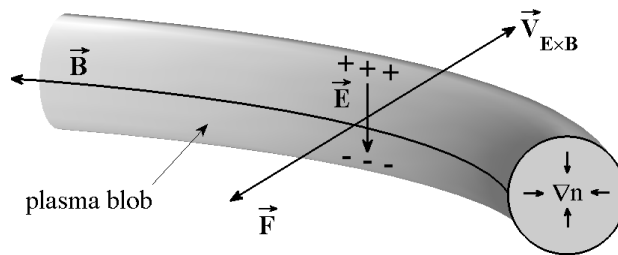


FIG. 1. Basic physics of plasma blobs driven by charge polarizing forces.

Most published work has only considered 2D dynamics of blobs by using different closure schemes to model the parallel dynamics and thereby ignores the variation of blob parameters along the magnetic field line [1, 3, 5, 7, 9, 10, 12, 13]. However, this approach is only valid on time scales short compared to the time scale of 3D instabilities, such as drift waves, which can be comparable to the time scale of blob motion for a wide range of parameters typical for current and future plasma devices.

Whether or not drift wave could be expected to affect the dynamics of plasma blobs is

estimated in this work by comparing the maximum growth rate from a local linear analysis of the governing equations with the blob convective rate from 2D theory. The important aspects of this expression are supported by a direct comparison of 2D and 3D seeded blob simulations using the code BOUT++ [16, 17].

The basic dynamics of blobs can be captured by solving the plasma vorticity and density equations for cold ions, isothermal electrons, and neglecting parallel ion dynamics. Under these assumptions, the following equations governing blobs driven by effective gravity forces are obtained from the conservation of charge and quasi-neutrality in a strongly magnetized plasma [10, 13]:

$$en\rho_s^2 \frac{d}{dt} \nabla_\perp^2 \frac{e\phi}{T_e} = \nabla_\parallel J_\parallel - \frac{eg}{\Omega_i} \frac{\partial n}{\partial y}, \quad (1)$$

$$\frac{d}{dt} n = \frac{1}{e} \nabla_\parallel J_\parallel - \frac{g}{\Omega_i} \frac{\partial n}{\partial y}, \quad (2)$$

where $\rho_s = c_s/\Omega_i$, $c_s = \sqrt{T_e/M_i}$, J_\parallel is the current density along the magnetic field, $\frac{d}{dt} = \frac{\partial}{\partial t} + \mathbf{V}_E \cdot \nabla$, $\mathbf{V}_E = c\mathbf{B} \times \nabla\phi/B^2$, g is the effective single particle gravitational acceleration [10], and all other parameters are defined conventionally with respect to cgs units. Some common examples of g are: magnetic field curvature and gradient forces $g_\kappa = 2c_s^2/R_c$ in the outer midplane of tokamaks with radius of curvature R_c , the effective centrifugal force $g_{cent} = V_\theta^2/a$ in linear plasma devices of radius a rotating with velocity V_θ [18], and the neutral wind force $g_{nw} = v_n\nu_{in}$ where v_n is the neutral velocity and ν_{in} is the ion-neutral collision frequency [19]. In terms of ion dynamics, the RHS of Eq. 2 represents the contribution of the ion polarization drift and is typically neglected in 2D theory since it is lower order than the $\mathbf{E} \times \mathbf{B}$ advection. However, this term has the important effect of making the drift wave instability well behaved in k-space and must be retained for 3D simulations.

The parallel current density is governed by Ohm's law: $J_\parallel = \sigma_\parallel T_e/e \nabla_\parallel (\ln(n) - e\phi/T_e)$, where $\sigma_\parallel = ne^2\tau_{ei}/(0.51m_e)$ is the plasma conductivity and $\tau_{ei} = 0.3m_e^2v_e^{3/2}/(ne^4\ln\Lambda)$ is the electron-ion collision time with $\ln\Lambda \approx 10$ and $v_e = \sqrt{T_e/m_e}$. For sheath connected blobs, J_\parallel from Ohm's law is matched to the current density from linear sheath theory at the parallel boundaries $z = \pm L/2$: $J_{\pm sh} = \pm\sigma_{\pm sh}\phi_{\pm sh}/(L/2)$, where $\sigma_{\pm sh} = c_sn_{\pm sh}e^2L/(2T_e)$ is the effective sheath conductivity and $n_{\pm sh}$ ($\phi_{\pm sh}$) is the density (potential) at the upper(+) and lower(-) sheaths. $\phi_{\pm sh}$ is taken with respect to the floating potential $\phi_f \approx 3T_e/e$ [10].

Plasma blobs are typically represented analytically by a Gaussian density profile in the drift plane with an amplitude on the order of or larger than the background density which

is usually taken as uniform. An exact linear analysis of the governing equations with this density profile is difficult since the effective gravity force combined with the poloidal density gradient does not satisfy a steady state solution of the governing equations. However, the dominant unstable modes will be shown to occur at $k_{\perp}\rho_s \approx 1$; whereas blobs are typically an order of magnitude larger than ρ_s . Thus, a standard local linear analysis of the governing equations by assuming an exponentially decaying background density with a characteristic scale length δ in the x-direction to be representative of the blob radius is sufficient to understand the effect of drift waves on blob dynamics. Perturbations of the form $(\tilde{n}, \tilde{\phi}) = (\hat{n}(z), \hat{\phi}(z))\exp(ik_y y - i\omega t)$ that satisfy the sheath boundary conditions are assumed. The sheath boundary conditions were found to be insignificant for parallel mode number $m \neq 0$ in the limit $k_{\parallel} \gg \sqrt{m_e/M_i}/\lambda_e$ where $\lambda_e = \tau_{ei}v_e/0.51$ the electron mean free path and $k_{\parallel} = \pi m/L$. The linear dispersion relation in this limit is found to be

$$\omega^2 + \omega_g^2 - \omega \frac{g\chi}{c_s} = -i\omega_{sh}\omega, \quad \text{for } m = 0 \quad (3)$$

$$\omega^2 + \omega_g^2 - \omega \frac{g\chi}{c_s} = -i\omega_{\parallel} [\omega - \omega_D], \quad \text{for } m = 1, 2, \dots \quad (4)$$

where $\chi = \rho_s k_y$, $\omega_g = \sqrt{g/\delta}$ is the flute mode frequency, $\omega_D = c_s\chi/(\delta(1 + \chi^2))$ is the drift frequency, $\omega_{sh} = \nu_{sh}/\chi^2$, $\nu_{sh} = 2c_s/L$ is the characteristic rate for parallel losses to the sheaths, $\omega_{\parallel} = \nu_{\parallel}(1 + \chi^2)/\chi^2$, and $\nu_{\parallel} = v_e\lambda_e k_{\parallel}^2$ is the characteristic rate for electrons to diffuse a distance on the order of a parallel wavelength. Even values of m correspond to even modes and odd values of m correspond to odd modes. The time scale for a blob to move a distance on the order of the blob size from 2D theory is ω_g^{-1} [10]. Eq. 3 is the 2D sheath mode and the growth rate is never larger than ω_g . Seeking growth rates from Eq. 4 large compared to ω_g , the maximum growth rate is found to be

$$\gamma_{max} \approx \frac{0.15c_s}{\sqrt{g\delta}}\omega_g. \quad (5)$$

This growth rate occurs at parallel and perpendicular wavelengths corresponding to $\omega_D \approx \omega_{\parallel}$ and $\chi \approx 1$ and suggests that blob transport may deviate from 2D theory due to drift waves when $0.15c_s/\sqrt{g\delta} \gtrsim 1$.

To numerically investigate the effect of drift waves on blob dynamics and make comparisons with 2D theory we first introduce the following non-dimensional transformation: $(x, y) \rightarrow \delta(x, y)$, $z \rightarrow (L/2)z$, $t \rightarrow \omega_g^{-1}t$, $\phi \rightarrow \sqrt{g\delta^3/(c_s\rho_s)^2}T_e\phi/e = \tilde{\phi}\phi$, $n \rightarrow \tilde{n}n$, and $J_{\parallel} \rightarrow e^2c_s\tilde{n}\tilde{\phi}/T_eJ_{\parallel}$. The dimensionless form of Eq. 1 and Eq. 2 along with parallel Ohm's

law are

$$n \frac{d}{dt} \nabla_{\perp}^2 \phi = \Delta^{\frac{5}{2}} \nabla_{\parallel} J_{\parallel} - \frac{\partial n}{\partial y}, \quad (6)$$

$$\frac{d}{dt} n = \frac{\rho}{\sqrt{\alpha \Delta}} \left(\Delta^{\frac{5}{2}} \nabla_{\parallel} J_{\parallel} - \frac{\partial n}{\partial y} \right), \quad (7)$$

$$J_{\parallel} = \sigma \nabla_{\parallel} \left(\frac{\rho}{\sqrt{\alpha^3 \Delta^3}} \ln(n) - \phi \right), \quad (8)$$

where $\rho \equiv g\rho_s/c_s^2$, $\sigma \equiv n_{sh}\sigma_{\parallel}/\sigma_{sh} = n\lambda_e\sqrt{M_i/m_e}/(L/2)$, $\alpha \equiv g\delta_*/c_s^2$, $\Delta \equiv \delta/\delta_*$, and $\delta_* \equiv \rho_s(gL^2/(4c_s^2\rho_s))^{1/5}$ is the fundamental size for coherently propagating blobs from 2D theory [7, 10]. The sheath boundary conditions in the dimensionless representation are $J_{\parallel}(z = \pm 1) = \pm n_{\pm}\phi_{\pm}$.

The evolution of the parallel gradients are set by σ . If $\sigma/n_{sh} \gg 1$ (which physically means that the resistance to the charge flow from the sheath potential is much stronger than the collisional resistance in the bulk of the plasma) and the density is initially uniform along B , then the potential drop between the sheaths can be neglected. This is the 2D limit and the divergence of J_{\parallel} can be shown to reduce to $\nabla_{\parallel} J_{\parallel} = n\phi$ [1, 10]. Furthermore, since the RHS of Eq. 7 is lower order than the $E \times B$ advection, it is seen that Δ is the main dimensionless parameter governing the 2D dynamics: blobs with $\Delta < 1$ are subject to the Kelvin-Helmholtz instability, blobs with $\Delta > 1$ have a convective time scale longer than ω_g^{-1} by a factor of $\Delta^{5/2}$ and break apart via the interchange instability from modes smaller than the blob, and the interchange and Kelvin-Helmholtz modes balance each other when $\Delta \sim 1$ and the blob can propagate relatively large radial distances as a coherent structure [3, 7, 10, 20].

To demonstrate the effect of drift waves on blob dynamics we reduce our attention to curvature and gradient driven blobs ($g = 2c_s^2/R_c$) and make direct comparisons of 2D and 3D simulation results from solving Eqs. 6-8 for the evolution of seeded blobs with BOUT++. The 2D operator $\nabla_{\parallel} J_{\parallel} = n\phi$ is used for the 2D simulations. Contours representing the blob density in the drift plane are presented with the 2D contours from the 3D simulations representing the density averaged along B . In all simulations, the background density n_0 is uniform and the blob density n_B is seeded on top of this background with twice the amplitude of the background, a constant profile along B , and a Gaussian profile in the drift plane with Gaussian width δ . The color code used in the contour plots is with respect to the background plasma density n_0 . $L = 10R_c$ was used in all simulations since the parallel

scale length in tokamaks is typically $L \approx q\pi R_c$ with safety factor $q \approx 3$.

Assuming the blob density is initially homogeneous along B may not always be a valid assumption for blobs in the scrape off layer of tokamaks owing to the strong ballooning characteristic of plasma turbulence [9]. However, this is what is assumed in 2D theory which we are attempting to make comparisons with. It is important to mention that the onset of unstable drift waves is delayed in our simulations due to the oversimplification of the initially flat density profile along B . The perturbations are not seeded, rather they are allowed to develop naturally during the blob propagation. Furthermore, the initial symmetry along the field line means that only even parallel modes will occur.

γ_{max}/ω_g scales with $\sqrt{R_c/\delta}$ for curvature and gradient driven blobs and thus only depends on the size of the blob and the radius of curvature of the system. To see the effects of drift waves on different size blobs we assume parameters typical of the edge region for current tokamaks: $T_e = 20$ eV, $B = 3$ T, $n_0 = 3 \times 10^{12}$ cm $^{-3}$, $R_c = 150$ cm, and $A = 2$ for the atomic number of deuterium. The results of 2D and 3D simulations for $\Delta = 1$ are shown in Fig. 2. The maximum normalized growth rate for these parameters is $\gamma_{max}/\omega_g \approx 2.4$. The 2D blob (top) remains coherent while travelling several blob widths, as is expected from 2D blob theory for $\Delta = 1$. The averaged density along the field line from the corresponding 3D simulation (bottom) matches well with the 2D theory at early stages in the 2D convection, but the onset of drift waves may be seen by looking at the individual slices along the field line shown in Fig. 3. At later times the 3D simulation yields a blob that is much more diffuse with a greatly reduced radial velocity in comparison to the 2D simulation. The mode numbers in the region of γ_{max} are $m = 4, 6$ which were also the dominant modes identified in the simulation.

2D and 3D simulations for $\Delta = 0.3$ are shown in Fig. 4 with all other parameters the same as was used in Fig. 2. Here we see the effects of drift waves at an earlier normalized time than for $\Delta = 1$, in correspondence with Eq. 5 which gives a maximum normalized growth rate $\gamma_{max}/\omega_g \approx 4.5$ and mode number $m = 8$. The dominant mode in the simulation was identified as $m = 8$.

To demonstrate that drift waves affect blobs at relatively earlier stages in the 2D convection in systems with a larger radius of curvature we choose edge parameters that may be typical for future tokamaks such as ITER: $T_e = 50$ eV, $B = 4$ T, $n_0 = 10^{13}$ cm $^{-3}$, and $R_c = 800$ cm. The results of the 2D simulation shown in Fig. 5 are practically identical to

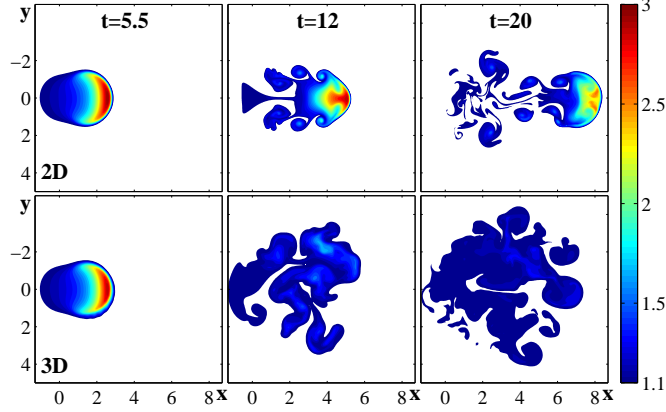


FIG. 2. Time slices of density contours from 2D simulation (top) and 3D simulation (bottom) for $\Delta = 1$, $\rho = 2.87 \times 10^{-4}$, $\sigma = 32.3$, and $\alpha = 3.68 \times 10^{-3}$.

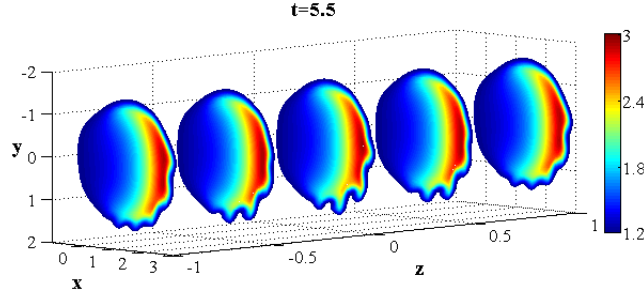


FIG. 3. 2D density contours from 3D simulation taken at different slices along the magnetic field line corresponding to the averaged density contour shown at $t=5.5$ in Fig. 2.

those in Fig. 4, as expected from 2D theory, but the onset of drift waves is noticeable at an earlier stage in the 3D simulation shown in Fig. 5 than it is in Fig. 4.

In summary, it is demonstrated that 2D blob theory holds well on time scales short compared to the growth time of unstable drift waves, but the free energy source present in the blob density gradient that drives the blob radially outward is quickly depleted during the nonlinear stage of unstable drift waves. The importance of resistive drift waves on blob dynamics is estimated by comparing the maximum linear growth rate from a standard local analysis of the blob equations with the 2D convective rate. The standard local linear analysis captures the dominant modes well since they occur for $k_{\perp}\rho_s \approx 1$; whereas the fundamental blob size δ_* is typically an order of magnitude larger than ρ_s . Furthermore, the same parameter limit originally considered for the validity of 2D blob theory ($\sigma_{\parallel} \gg \sigma_{sh}$)

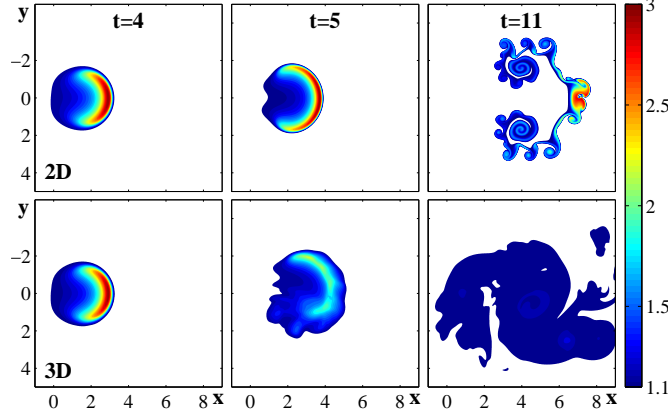


FIG. 4. Time slices of density contours from 2D simulation (top) and 3D simulation (bottom) for $\Delta = 0.3$, $\rho = 2.87 \times 10^{-4}$, $\sigma = 32.3$, and $\alpha = 3.68 \times 10^{-3}$.

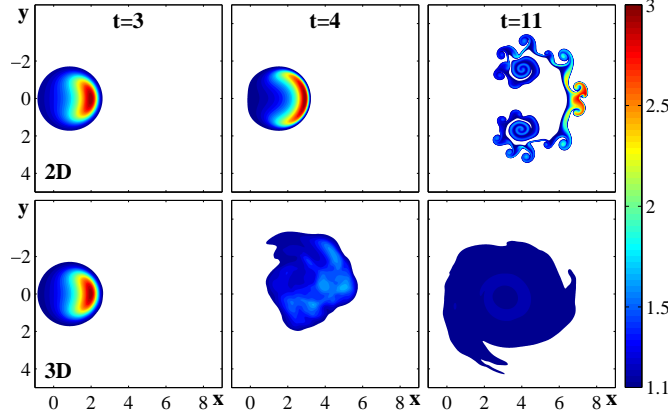


FIG. 5. Time slices of density contours from 2D simulation (top) and 3D simulation (bottom) for $\Delta = 0.3$, $\rho = 6.4E - 5$, $\sigma = 11.4$, and $\alpha = 1.1 \times 10^{-3}$.

may also be used to ignore the effect of the sheath boundary conditions on the parallel modes for $m \neq 0$. Interestingly, this parameter does not enter directly into the maximum growth rate. However, it does enter indirectly by affecting what parallel mode number the maximum growth rate will occur. This is determined by $\omega_{\parallel} \approx \omega_D$ and in the limit as $\sigma_{\parallel}/\sigma_{sh} \rightarrow \infty$, the parallel modes in the region of the maximum growth rate cannot be supported in a finite system and 2D theory should be valid with respect to the drift wave instability. However, for parameters typical of most linear and toroidal devices, the modes corresponding to $\omega_{\parallel} \approx \omega_D$ can be supported.

For magnetic field curvature and gradient driven blobs, Eq. (5) suggests that drift waves could be important for all blobs with $\delta \lesssim R_c/100$, which is typical for current and future

tokamaks and should therefore be addressed in blob theory and modeling. The growth rate is relatively larger for smaller blobs and this could explain why the detailed mushrooming of small blobs described by 2D theory and seen in 2D simulations [7, 9, 10] is never actually seen in experiments [13]. Also, the radial distance the blobs travel as a coherent structure is less in systems with a smaller effective gravity force. This could be beneficial for limiting particle and heat flux to the first wall for future tokamak reactors such as ITER.

Ignoring parallel ion dynamics in the density evolution is justified since $c_s k_{\parallel} < \omega_g$ and the time scales of the simulations presented are small compared to the parallel loss time $L\omega_g/(2c_s)$. However, the use of parallel Ohm's law is only valid in the collisional fluid limit where $\lambda_e k_{\parallel} < 1$ and this parameter is marginal for most current and future tokamak edge parameters. Also, to treat electrons isothermally in the collisional limit requires $\omega < \nu_{\parallel}$, but the maximum growth rate was found to occur when $\omega \approx \omega_D \sim \nu_{\parallel}$. Furthermore, although the ions are typically much colder than the electrons in the edge of most small scale experimental devices, it can be comparable to or even larger than T_e in the edge region of tokamaks [13]. In this situation, k_{\perp}^{-1} corresponding to the dominant unstable drift wave modes become comparable to the ion gyro-radius. All of these limitations should be considered when interpreting the results of this paper and they suggest that kinetic effects may play an important role on blob dynamics.

Electrostatic drift wave turbulence is known to saturate to a self-organized state under certain circumstances [21]. It was found in this study that, for certain parameter sets, the blob potential does saturate to a self-organized state resulting in a diffuse blob rotating about a central axis in the drift plane. However, for other parameters, this self-organized state was not found. A better understanding of the non-linear saturated state of plasma blobs that undergo drift wave turbulence and drawing connections with known theories on self-organization of electrostatic potential is a topic for future research.

Research supported by USDOE grant DE-FG02-04ER54739 and used resources of the National Energy Research Scientific Computing Center, which is supported by the Office of Science of the U.S. Department of Energy under Contract No. DE-AC02-05CH11231.

[1] S. Krasheninnikov, Physics Letters A **283**, 368 (2001).

[2] J. Boedo, D. Rudakov, R. Moyer, S. Krasheninnikov, D. Whyte, G. McKee, G. Tynan,

- M. Schaffer, P. Stangeby, P. West, *et al.*, Physics of Plasmas **8**, 4826 (2001).
- [3] G. Yu and S. Krasheninnikov, Physics of Plasmas **10**, 4413 (2003).
 - [4] D. Russell, D. D'Ippolito, J. Myra, W. Nevins, and X. Xu, Physical review letters **93**, 265001 (2004).
 - [5] J. Myra, D. D'Ippolito, S. Krasheninnikov, and G. Yu, Physics of plasmas **11**, 4267 (2004).
 - [6] O. Garcia, V. Naulin, A. Nielsen, and J. Rasmussen, Physical review letters **92**, 165003 (2004).
 - [7] A. Aydemir, Physics of plasmas **12**, 062503 (2005).
 - [8] D. Rudakov, J. Boedo, R. Moyer, N. Brooks, R. Doerner, T. Evans, M. Fenstermacher, M. Groth, E. Hollmann, S. Krasheninnikov, *et al.*, Journal of nuclear materials **337**, 717 (2005).
 - [9] O. Garcia, N. Bian, and W. Fundamenski, Physics of plasmas **13**, 082309 (2006).
 - [10] S. Krasheninnikov, D. D'Ippolito, and J. Myra, J. Plasma Phys **74** (2008).
 - [11] I. Furno, B. Labit, M. Podestà, A. Fasoli, S. Müller, F. Poli, P. Ricci, C. Theiler, S. Brunner, A. Diallo, *et al.*, Physical review letters **100**, 55004 (2008).
 - [12] O. Garcia, Plasma and Fusion Research **4**, 19 (2009).
 - [13] D. D'Ippolito, J. Myra, and S. Zweben, Physics of Plasmas **18**, 060501 (2011).
 - [14] P. Manz, M. Xu, S. Müller, N. Fedorczak, S. Thakur, J. Yu, and G. Tynan, Physical Review Letters **107**, 195004 (2011).
 - [15] C. Theiler, I. Furno, J. Loizu, and A. Fasoli, Physical Review Letters **108**, 065005 (2012).
 - [16] B. Dudson, M. Umansky, X. Xu, P. Snyder, and H. Wilson, Computer Physics Communications **180**, 1467 (2009).
 - [17] M. Umansky, X. Xu, B. Dudson, L. LoDestro, and J. Myra, Computer Physics Communications **180**, 887 (2009).
 - [18] P. Popovich, M. Umansky, T. Carter, and B. Friedman, Physics of Plasmas **17**, 2107 (2010).
 - [19] S. Krasheninnikov and A. Smolyakov, Physics of Plasmas **10**, 3020 (2003).
 - [20] N. Bian, S. Benkadda, J. Paulsen, and O. Garcia, Physics of Plasmas **10**, 671 (2003).
 - [21] A. Hasegawa and M. Wakatani, Physical review letters **59**, 1581 (1987).